International Journal of Naval Architecture and Ocean Engineering 11 (2019) 865–874

Contents lists available at ScienceDirect

International Journal of Naval Architecture and Ocean Engineering

journal homepage: http://www.journals.elsevier.com/international-journal-of-naval-architecture-and-ocean-engineering/

A controller comprising tail wing control of a hybrid autonomous underwater vehicle for use as an underwater glider

Moon G. Joo

Department of Information and Communications Engineering, Pukyong National University, 45 Yongso-ro, Nam-gu, Busan, Republic of Korea

ARTICLE INFO

Article history:
Received 28 September 2018
Received in revised form
21 January 2019
Accepted 6 March 2019
Available online 8 March 2019

Keywords:
Underwater glider
Luenberger observer
PD
LQR

ABSTRACT

A controller for an underwater glider is presented. Considered underwater glider is a torpedo-shaped autonomous underwater vehicle installing adjustable buoyancy bag and movable battery in it. The controller is composed of an LQR controller to maintain zigzag vertical movement for gliding and two PD controllers to control elevator/rudder angles. The LQR controller controls the pumping speed into the buoyancy bag and the moving speed to locate the battery. One of the PD controller controls the elevator angle to assist the LQR controller, and the other controls the rudder angle to adjust the direction of the underwater glider. A reduced order Luenberger observer is adopted to estimates the center of gravity of the glider and the buoyancy mass that are essential but cannot be measured. Mathematical simulation using Matlab proved the validity of the proposed controller to obtain better performance than conventional LQR only controller under the influence of sea current.

1. Introduction

Unmanned Underwater Vehicle (UUV), also known as underwater drone, can be roughly grouped into Remotely Operated Vehicle (ROV), Autonomous Underwater Vehicle (AUV), and underwater glider.

ROV (Ballard, 1993; Javadi-Moghaddam and Bagheri, 2010; Shim et al., 2010) receives power through the power line connected from a mother ship on the sea, and its movement are controlled remotely using the connected tether line by operators in the mother ship. Because it can hover at a designated point by using several propellers, for example, forward/backward, left/right, and up/down propellers, it can perform sophisticatee tasks with attached robot arms without losing balance. The range of activity is limited to the length of the tether line.

AUV (Presto, 2001; Hagen et al., 2008; Jun et al., 2009) has mostly torpedo shape and has a wide range of activity because it operates with its own battery and control system without tether line from mother ship. It is used for underwater mine search or exploration of undersea topography. Due to the use of propeller propulsion causing high battery consumption, its operating time is limited to within a few hours. To overcome this problem, large scale AUVs with large capacity batteries and AUVs using fuel cells are being developed.

Underwater glider (Alvarez, 2010; Webb et al., 2001; Eriksen et al., 2001; Sherman et al., 2001) has its own battery and control system like AUV. Instead of using battery-driven propeller propulsion system, it advances through a zigzag motion in up/down direction using controllable buoyancy device and center-of-gravity movement device installed inside. Because it consumes much less energy than AUV, underwater glider can operate for more than one month. However, the turning radius is too large to search or control precisely. It is used to search the seabed salinity distribution, temperature distribution, and so on.

On the other hand, Hybrid AUV (HAUV) (Joo and Qu, 2015) with a gliding function was proposed by modifying the existing AUV and installing a battery and a buoyancy control device in it. The HAUV can glide to the distant ocean with small energy until near the target point. And it performs precise search operations using the propeller and its tail wings like as conventional AUV. In (Joo and Qu, 2015), an LQR controller was proposed to control the center of gravity and the buoyant mass inside the HAUV so that it can perform the gliding function. In (Joo et al., 2017), a method of calculating the center of gravity and the buoyancy mass, which can not be directly measured, was proposed, where a reduced order observer was used for the LQR controller.

This paper deals with the use of rudders (vertical tail wings) and elevators (horizontal tail wings) that HAUV did not use when

E-mail address: gabi@pknu.ac.kr.
Peer review under responsibility of Society of Naval Architects of Korea.

https://doi.org/10.1016/j.ijnaoe.2019.03.001

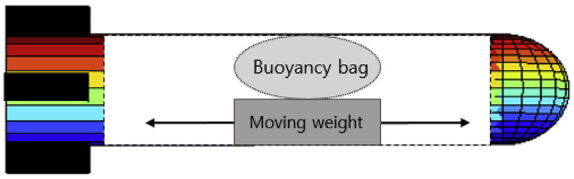

Fig. 1. HAUV model with a moving mass and a adjustable buoyancy bag.

operating as a glider. The proposed controller controls the rudder angle to move to the desired direction and the elevator angle to assist the vertical zigzag motion of HAUV, while LQR controller controls the buoyancy mass and center of gravity.

The controller consists of a conventional LQR controller and two PID controllers for controlling rudders and elevators. A reduced order state observer is adopted to calculate the center of gravity and buoyancy mass. With the proposed control scheme, the HAUV is shown to overcome the influence of sea current and to move to designated directions when operating as underwater glider.

It is worth mentioning another study that combines the merits of AUV and underwater glider. The underwater glider with a thruster (Wang et al., 2011; Xue et al., 2018) is most similar to the proposed HAUV. However, they used the thruster to maintain the zigzag motion of glider under strong sea current. To adjust the direction, they did not use rudders but rotate the battery pack like a conventional underwater glider. In other words, the underwater glider operates always as an underwater glider, even with a thruster and rudders.

2. Mathematical model of the considered HAUV (Joo and Qu, 2015)

The shape of the HAUV considered is shown in Fig. 1. Inside the HAUV, a battery pack moves forward and backward to control the center of gravity of the HAUV. An adjustable buoyancy bag is set to control the buoyancy of the HAUV.

As is well known, the six degrees of freedom motion of an underwater robot can be represented by nonlinear differential equations with twelve parameters, $(x, y, z, u, v, w, \phi, \theta, \psi, p, q, r)$ as shown in Fig. 2 (Fossen, 1994, 2011). The NED coordinate is used as the earth fixed coordinate system.

Generally, the center of buoyancy is the origin of the body fixed coordinate, i.e., $(x_b, y_b, z_b) = 0$. The center of gravity in each direction is denoted as (x_g, y_g, z_g). The mass of the vehicle is

$$m_v = m_h + \overline{m} + m_b$$

where m_h is the mass of hull and its static components, $\overline{m}$ is the moving mass such as battery pack, and m_b is the point mass buoyancy.

Dynamic equations of HAUV are given as follows, where I_{xx}, I_{yy} and I_{zz} are moments of inertia in the body fixed coordinate and $\sum X_{ext}, \sum Y_{ext}, \sum Z_{ext}, \sum K_{ext}, \sum M_{ext}$ and $\sum N_{ext}$ are external forces and momentums.

$$m_v\left[\dot{u} - vr + wq - x_g\left(q^2 + r^2\right) + y_g(pq - \dot{r}) + z_g(pr + \dot{q})\right] = \sum X_{ext}$$

$$m_v\left[\dot{v} - wp + ur - y_g\left(r^2 + p^2\right) + z_g(qr - \dot{p}) + x_g(qp + \dot{r})\right] = \sum Y_{ext}$$

$$m_v\left[\dot{w} - uq + vp - z_g\left(p^2 + q^2\right) + x_g(rp - \dot{q}) + y_g(rq + \dot{p})\right] = \sum Z_{ext}$$

$$I_{xx}\dot{p} + (I_{zz} - I_{yy})qr + m_v\left[y_g(\dot{w} - uq + vp) - z_g(\dot{v} - wp + ur)\right] = \sum K_{ext}$$

$$I_{yy}\dot{q} + (I_{xx} - I_{zz})rp + m_v\left[z_g(\dot{u} - vr + wq) - x_g(\dot{w} - uq + vp)\right] = \sum M_{ext}$$

$$I_{zz}\dot{r} + (I_{yy} - I_{xx})pq + m_v\left[x_g(\dot{v} - wp + ur) - y_g(\dot{u} - vr + wq)\right] = \sum N_{ext}$$

The notations ξ, α, and θ in Fig. 3 are associated with angles and mean the flight angle, the attack angle, and the pitch angle, respectively. The notations V, u, and w are associated with

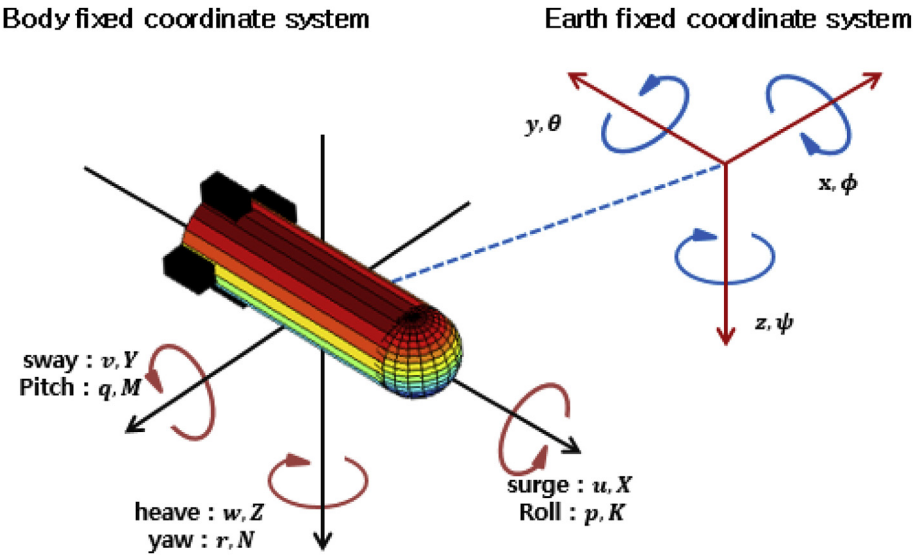

Fig. 2. State variables represented in the body fixed coordinate system and the Earth fixed coordinate system.

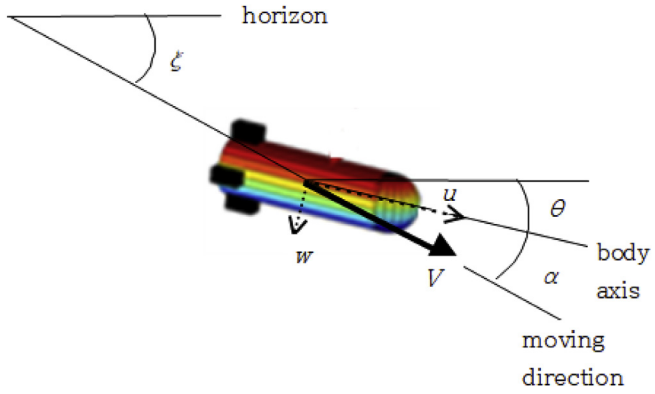

Fig. 3. Flight angle (ξ), attack angle (α), and pitch angle (θ).

velocities and mean the moving speed, the surge, and the heave, respectively.

According to (Joo and Qu, 2015), the conditions for stable gliding for HAUV are summarized in Table 1. The moving speed (V_d) and the desired flight angle (ξ_d) are two design factors. Once they are chosen, the remainder is calculated from mathematical model of the HAUV and the assumption that the lateral movement does not occur in the stable gliding. V_d is set to 0.3 m/s arbitrarily. Since the HAUV considered does not have wings, too small flight angle does not match the stable gliding and three ξ_d are considered, which are ±30°, ±45°, and ±60°.

For the mathematical model of HAUV, REMUS is assumed to be the existing AUV and its known coefficients are adopted. The notations x_g and m_b are the center of gravity in x axis and the buoyancy mass, respectively. The subscript d represents the desired target value.

3. Reduced order state observer (Joo et al., 2017)

According to (Joo and Qu, 2015), the continuous-time state equation for depth control of the HAUV is linearized as shown in the following equations, beside the operating points.

$$\Delta\dot{X} = \tilde{A}\Delta X + \tilde{B}U, \tag{1}$$

where

$$\Delta X = X - X_d$$

$$X = \begin{bmatrix} u\ w\ q\ z'\ \theta\ x_g\ m_b \end{bmatrix}^T$$

$$X_d = \begin{bmatrix} u_d\ w_d\ 0\ 0\ \theta_d\ x_{gd}\ m_{bd} \end{bmatrix}^T,$$

$$U = [\,u_x \quad u_b\,]^T$$

$$M = \begin{bmatrix} m_{v0} - X_{\dot{u}} & 0 & m_{v0}Z_G & 0 & 0 & 0 & 0 \\ 0 & m_{v0} - Z_{\dot{w}} & -\left(m_{v0}x_g + Z_{\dot{q}}\right) & 0 & 0 & 0 & 0 \\ m_{v0}Z_G & -\left(m_{v0}x_g + M_{\dot{w}}\right) & I_{yy} - M_{\dot{q}} & 0 & 0 & 0 & 0 \\ 0 & 0 & 0 & 1 & 0 & 0 & 0 \\ 0 & 0 & 0 & 0 & 1 & 0 & 0 \\ 0 & 0 & 0 & 0 & 0 & 1 & 0 \\ 0 & 0 & 0 & 0 & 0 & 0 & 1 \end{bmatrix},$$

$$A = \begin{bmatrix} 0 & 0 & (Z_{\dot{w}} - m_{vd})w_d & 0 & -(W_d - B)\cos\theta_d & 0 & -g\sin\theta_d \\ Z_{uw}w_d & Z_{uw}u_d & (m_{vd} + Z_{uq})u_d & 0 & -(W_d - B)\sin\theta_d & 0 & g\cos\theta_d \\ M_{uw}w_d & M_{uw}u_d & a_{33} & 0 & a_{35} & -W_d\cos\theta_d & 0 \\ -\sin\alpha_d & \cos\alpha_d & 0 & 0 & a_{45} & 0 & 0 \\ 0 & 0 & 1 & 0 & 0 & 0 & 0 \\ 0 & 0 & 0 & 0 & 0 & 0 & 0 \\ 0 & 0 & 0 & 0 & 0 & 0 & 0 \end{bmatrix},$$

$$a_{33} = \left(M_{uq} - m_{vd}x_{gd}\right)u_d - m_{vd}Z_G w_d,$$
$$a_{35} = \left(-Z_G\cos\theta_d + x_{gd}\sin\theta_d\right)W_d,$$
$$a_{45} = -u_d\cos\alpha_d - w_d\sin\alpha_d,$$

Table 1
Desired values of parameters for stable gliding.

	downward			upward		
ξ_d(deg)	−30°	−45°	−60°	30°	45°	60°
α_d(deg)	12°	7°	4°	−12°	−7°	−4°
θ_d(deg)	−18°	−38°	−56°	18°	38°	56°
V_d(m/s)	0.30	0.30	0.30	0.30	0.30	0.30
u_d(m/s)	0.2936	0.2978	0.2993	0.2936	0.2978	0.2993
w_d(m/s)	0.0615	0.0364	0.0209	−0.0615	−0.0364	−0.0209
x_{gd}(m)	0.0080	0.0167	0.0305	−0.0080	−0.0167	−0.0305
m_{bd}(kg)	0.9436	0.8954	0.8778	0.7262	0.7743	0.7919

$$B = \begin{bmatrix} 0 & 0 \\ 0 & 0 \\ 0 & 0 \\ 0 & 0 \\ 0 & 0 \\ b_x & 0 \\ 0 & b_m \end{bmatrix},\quad F = \begin{bmatrix} X_{op} \\ Z_{op} \\ M_{op} \\ q_{op} \\ z'_{op} \\ x_{g.op} \\ m_{b.op} \end{bmatrix},\quad C = \begin{bmatrix} 1 & 0 & 0 & 0 & 0 & 0 & 0 \\ 0 & 1 & 0 & 0 & 0 & 0 & 0 \\ 0 & 0 & 1 & 0 & 0 & 0 & 0 \\ 0 & 0 & 0 & 1 & 0 & 0 & 0 \\ 0 & 0 & 0 & 0 & 1 & 0 & 0 \end{bmatrix},$$

$$\tilde{A} = M^{-1}A,$$
$$\tilde{B} = M^{-1}B,$$
$$\tilde{F} = M^{-1}F.$$

Here, the output of the controller u_x and u_b mean the motor speed

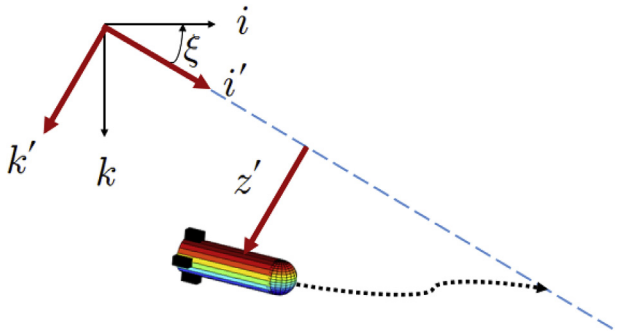

Fig. 4. Vertical distance from trajectory.

to move the battery and the pumping speed to inflate/deflate the buoyancy bag, respectively. The state variables required for HAUV control are the surge (u), heave (w), pitch rate (q), vertical distance from trajectory (z'), pitch (θ), center of gravity in forward direction (x_g), and buoyancy mass (m_b). The variable, z', means the perpendicular distance from the desired trajectory as shown in Fig. 4. The purpose of depth control is to make z' as 0.

Unlike the previous five state variables, which can be directly measured by sensors, for example, IMU, DVL, and depth sensor, the center of gravity and the buoyancy mass can not be measured, so a mathematical observer is needed to estimate them. A discrete time reduced order Luenberger state observer proposed in (Joo et al., 2017) is adopted to estimate x_g and m_b.

The linearized continuous-time state Eq. (1) is converted to the discrete-time state equation where A_d and B_d are obtained by zero-order-holder with sampling time T. The variable $y(1\times 5)$ means five measured values and $w(1\times 2)$ means values to be estimated.

$$\Delta X(k+1) = A_d \Delta X(k) + B_d U(k) \tag{2}$$

$$A_d = \begin{bmatrix} A_{11}(5\times 5) & A_{12}(5\times 2) \\ A_{21}(2\times 5) & A_{22}(2\times 2) \end{bmatrix}$$
$$B_d = \begin{bmatrix} B_{11}(5\times 2) \\ B_{21}(2\times 2) \end{bmatrix}$$
$$\Delta X(k) = \begin{bmatrix} y(1\times 5) \\ w(1\times 2) \end{bmatrix}$$
$$U(k) = \begin{bmatrix} u_x \\ u_b \end{bmatrix}$$

Rewriting (2) as

$$y(k+1) = A_{11}y(k) + A_{12}w(k) + B_{11}U(k)$$
$$w(k+1) = A_{21}y(k) + A_{22}w(k) + B_{21}U(k),$$

and setting $v(k) = w(k) - Ly(k)$, we have

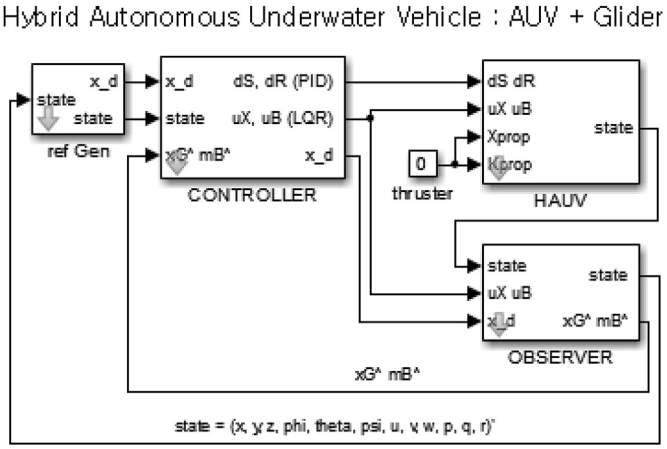

Fig. 5. Structure of the proposed controller.

$$v(k+1) = (A_{22} - LA_{12})v(k) + (A_{21} - LA_{11} + A_{21}L - LA_{11}L)y(k) + (B_{21} - LB_{11})U(k)$$

$$\hat{v}(k+1) = (A_{22} - LA_{12})\hat{v}(k) + (A_{21} - LA_{11} + A_{21}L - LA_{11}L)y(k) + (B_{21} - LB_{11})U(k),$$

where $\hat{v}(k)$ is an estimator of $v(k)$.

Error equation becomes

$$e(k) = v(k) - \hat{v}(k)$$
$$e(k+1) = (A_{22} - LA_{12})e(k)$$

and the error decays exponentially if $(A_{22} - LA_{12})$ is Hurwitz.

Now $w(1\times 2)$ consisting of x_g and m_b is obtained by

$$w(k) = \hat{v}(k) + Ly(k).$$

4. Proposed controrller of HAUV

Fig. 5 shows the structure of the proposed controller. In the simulation, propulsion (Xprop) and torque (Kprop) by propellers are set to 0 and it means that propellers of the HAUV are not used. xG and mB notates the estimated values of x_g and m_b, respectively.

The poles of the observer are set to $-20\pm j20$ in continuous complex domain and transformed to discrete time domain with $T = 1$. By using Matlab command 'place' which implents the pole placement technique, observer gain L is obtained as

$$L = \begin{bmatrix} 0.0047 & 0.0021 & -0.0250 & 0.0024 & -0.0139 \\ 3.2821 & 4.4789 & 0.3337 & 1.9493 & -0.2282 \end{bmatrix}$$ when HAUV goes down and

$$L = \begin{bmatrix} -0.0045 & 0.0034 & -0.0252 & 0.0031 & -0.0141 \\ -3.2914 & 4.4641 & 0.2781 & 1.9518 & -0.2626 \end{bmatrix}$$ when HAUV goes up.

The changes of the center of gravity (x_g) and buoynacy mass (m_b) are expressed by

$$\dot{x}_g = b_x u_x$$
$$\dot{m}_b = b_m u_b,$$

where b_x denotes the rate of change of center of gravity per input voltage u_x applying to the DC motor that moves the battery pack, and b_m denotes the rate of change of buoyancy mass per input voltage u_b applying to the buoyancy pump.

For vertical zigzag motion of HAUV, a digital LQR controller controls the buoyancy mass and the center of gravity. The control gains at the time of going up and down are obtained with the "dlqr" command from Matlab.

When HAUV is going down,

$$K = \begin{bmatrix} 0.1275 & -0.0477 & -0.0021 & -0.0009 & 0.0253 & 18.2924 & 0.4136 \\ 0.0685 & -0.0195 & -0.0021 & -0.0004 & 0.0110 & 6.9030 & 0.6220 \end{bmatrix}.$$

When HAUV is going up,

$$K = \begin{bmatrix} -0.1278 & -0.0481 & -0.0074 & -0.0009 & 0.0253 & 18.2666 & 0.4104 \\ -0.0683 & -0.0196 & -0.0049 & -0.0004 & 0.0109 & 6.8504 & 0.6195 \end{bmatrix}.$$

The LQR controller is of the form,

$$U(k) = -K\Delta X(k).$$

On the other hand, torpedo type AUVs such as REMUS have elevators, which can be used to adjust its depth during vertical zigzag moving. Since a small energy is enough to move the elevators, in this paper, we propose to use them in parallel with the LQR controller for depth control of HAUV gliding operation.

The effect of elevator angle (δs) is relected in $\sum Z_{ext}$ as

$$\begin{aligned} \sum Z_{ext} &= Z_{HS} && ;\textit{Hydro Static} \\ &+ Z_{\dot{w}}\dot{w} + Z_{\dot{q}}\dot{q} - X_{\dot{u}}uq + Y_{\dot{v}}vp + Y_{\dot{r}}rp && ;\textit{Added Mass, Coriolis} \\ &+ Z_{w|w|}w|w| + Z_{q|q|}q|q| && ;\textit{Crossflow Drag} \\ &+ Z_{uwl}uw && ;\textit{Body Lift} \\ &+ Z_{uu\delta s}u^2\delta s + Z_{uwf}uw + Z_{uqf}uq && ;\textit{Fin Lift}. \end{aligned}$$

The main contribution of this paper is to control the angle of the horizontal tail wings which was not used in the conventional gliding operation. We chose not to create a new LQR controller containing δs but to add an independent controller that can be used only when needed, while maintaining the existing LQR controller.

Selected controller is a simple PD controller configured as

$$\delta s(k) = -0.1e_{z'}(k) - 0.1\frac{e_{z'}(k) - e_{z'}(k-1)}{T}$$
$$e_{z'}(k) = z'(k),$$

where $z'(k)$ is the vertical distance from the trajectory and T is the sample time. The PD controller determines the elevator angle, δs, to make $z'(k)$ to 0.

Since the controller uses only the vertical distance and its derivative, it is simple and easy to adjust the gains. Despite the simple sturcture, however, the control performance is greatly improved compared to the conventional LQR controller as will be shown in simulations.

We also propose the use of rudders of HAUV to control the direction, since the torpedo type AUV has vertical tail wings, rudders.

As with the elevator control, a small energy is enough to move the rudders. The effect of rudder angle (δr) is relected in $\sum Y_{ext}$ as

$$\begin{aligned} \sum Y_{ext} &= Y_{HS} && ;\text{Hydro Static} \\ &+ Y_{\dot{v}}\dot{v} + Y_{\dot{r}}\dot{r} + X_{\dot{u}}ur - Z_{\dot{w}}wp - Z_{\dot{q}}pq && ;\text{Added Mass, Coriolis} \\ &+ Y_{v|v|}v|v| + Y_{r|r|}r|r| && ;\text{Crossflow Drag} \\ &+ Y_{uvl}uv && ;\text{Body Lift} \\ &+ Y_{uu\delta r}u^2\delta r + Y_{uvf}uv + Y_{urf}ur && ;\text{Fin Lift}. \end{aligned}$$

And the selected PD controller of the rudder is configured as

$$\delta r(k) = 0.05e_{\psi}(k) + 0.1\frac{e_{\psi}(k) - e_{\psi}(k-1)}{T}$$
$$e_{\psi}(k) = \psi_d(k) - \psi(k),$$

where ψ is the yaw angle. The PD controller determines the ruder angle, δr to make ψ to ψ_d.

Conventional method of direction control is a bank turn that rotates with a large raius by moving the battery position to the side of the travel direction to induce a roll change. However, this type of

Table 2
HAUV Parameters used for simulation (unit: MKS).

$m_h = 30.4791$	$x_b = 0$	$I_{xx} = 0.1770$
$\overline{m} = 1$	$y_b = 0$	$I_{yy} = 3.4500$
$m = 32.3140$	$z_b = 0$	$I_{zz} = 3.4500$
$g = 9.8100$	$x_g = 0$	
$b_x = 0.001$	$y_g = 0$	
$b_m = 0.017$	$z_g = 0.0200$	
$X_{\dot{u}} = -0.9300$	$Y_{v\|v\|} = -1310$	$Z_{w\|w\|} = -131$
$Z_{\dot{w}} = -35.5000$	$Y_{r\|r\|} = 0.6320$	$Z_{q\|q\|} = -0.6320$
$Z_{\dot{q}} = -1.9300$	$Y_{uvl} = -18.9600$	$Z_{uwl} = -18.9600$
$Y_{\dot{v}} = -35.5000$	$Y_{uu\delta r} = 9.6400$	$Z_{uu\delta s} = -9.6400$
$Y_{\dot{r}} = 1.9300$	$Y_{uvf} = -9.6400$	$Z_{uwf} = -9.6400$
$X_{u\|u\|} = -3.9000$	$Y_{urf} = 6.1500$	$Z_{uqa} = 0.9300$
		$Z_{uqf} = -6.1500$
$K_{\dot{p}} = -0.0704$	$M_{\dot{w}} = -1.9300$	$N_{\dot{v}} = 1.9300$
$K_{p\|p\|} = -0.1300$	$M_{\dot{q}} = -4.8800$	$N_{\dot{r}} = -4.8800$
	$M_{w\|w\|} = 3.1800$	$N_{v\|v\|} = -3.1800$
	$M_{q\|q\|} = -188$	$N_{r\|r\|} = -94$
	$M_{uwl} = -4.4200$	$N_{uvl} = 4.4500$
	$M_{uu\delta s} = -6.1500$	$N_{uu\delta r} = -6.1500$
	$M_{uwf} = -6.1500$	$N_{uvf} = 6.1500$
	$M_{uqf} = -3.9300$	$N_{urf} = -3.9300$

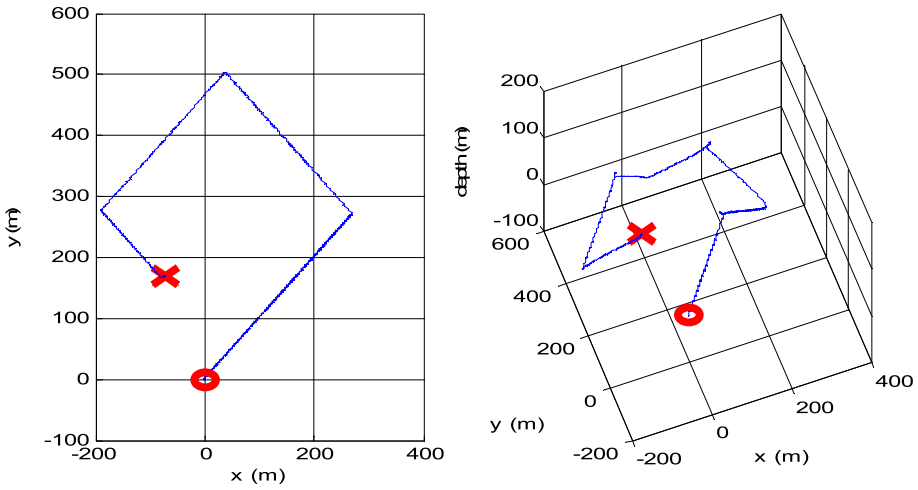

Fig. 6. The trajectory of HAUV with an LQR depth controller and a PID direction controller.

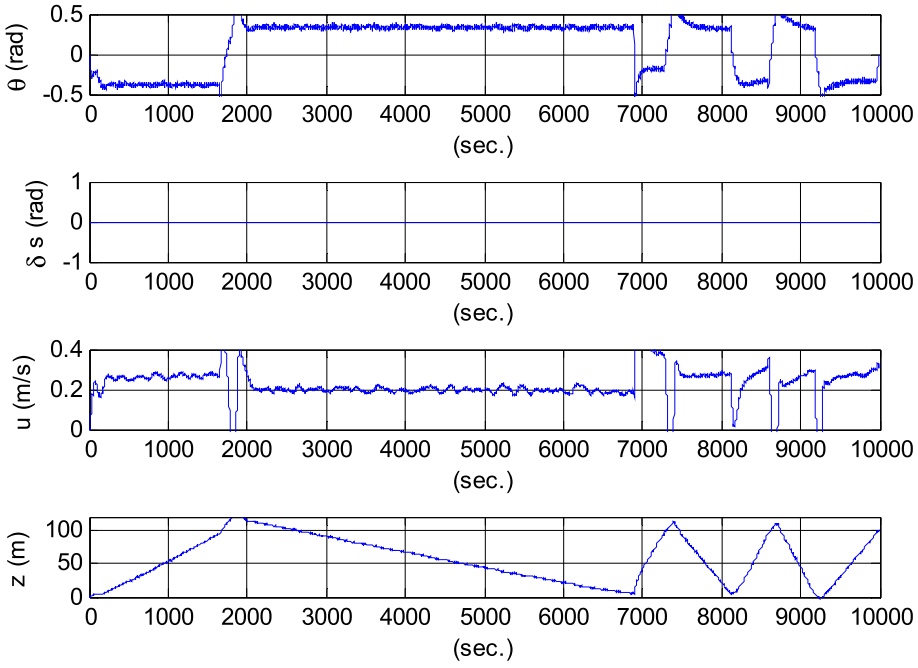

Fig. 7. Variables related to depth control by an LQR without elevator control.

direction control not only requires a complicated battery moving device, but also causes a large turning radius.

The proposed method has advantage that the direction change is only affected by the tail wing, not the battery position, and has a small turning radius too.

5. Simulation

To verify the performance of the proposed controller, Matlab simulation was performed under the same conditions as in (Joo and Qu, 2015; Joo et al., 2017). In this paper, we add the influence of oncoming sea current from northeast, which was not considered in the previous papers. In addition, we use the reduced order state observer proposed in (Joo et al., 2017) to calculate the center of gravity and the buoyancy mass while the paper (Joo and Qu, 2015) assumes that all state variables are known accurately. The proposed controller is composed of an LQR controller to maintain zigzag vertical movement and two PD controllers to control elevator angle and rudder angle

One target point consists of the desired depth and the direction, and the target trajectory is presented as follows using consecutive target points.

$$(0,0)\rightarrow\left(100,\frac{1}{4}\pi\right)\rightarrow\left(0,\frac{1}{4}\pi\right)\rightarrow\left(100,\frac{3}{4}\pi\right)\rightarrow\left(0,\frac{3}{4}\pi\right)\rightarrow\left(100,\frac{5}{4}\pi\right)\rightarrow\left(0,\frac{5}{4}\pi\right)\rightarrow\left(100,\frac{7}{4}\pi\right)\rightarrow\left(0,\frac{7}{4}\pi\right)\rightarrow(100,0)\rightarrow(0,0)$$

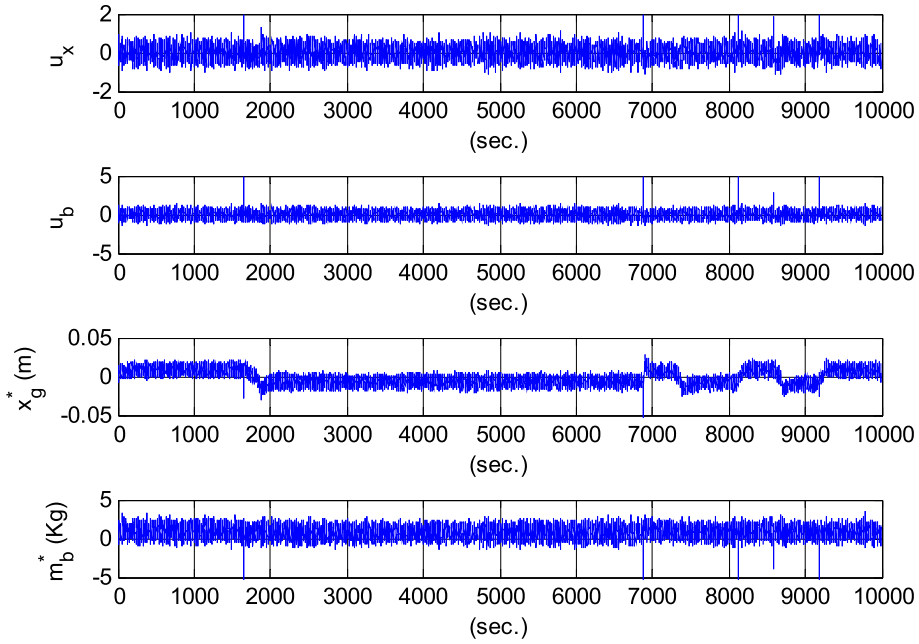

Fig. 8. Control effort of the LQR and changes of the estimated values.

In the simulation, the following reasonable measurement noises are added:

$$u_n, v_n, w_n : rand(-0.0051,\ 0.0051)\ \ ;\pm 0.01\ \text{knot (DVL)}$$
$$p_n, q_n, r_n : rand(-0.2618,\ 0.2618)\ \ ;\pm 15\ ^\circ/\text{sec (DVL)}$$
$$x_n, y_n, z_n : rand(-0.5000,\ 0.5000)\ \ ;\pm 0.5\ m\ \text{(GPS)}$$
$$\phi_n, \theta_n, \varphi_n : rand(-0.0175,\ 0.0175)\ \ ;\pm 1^\circ\ \text{(IMU)}$$

where $(\cdot)_n$ denotes the noise to each variable, and $rand(\ )$ denotes a random value within the given range. The values are dictated from the specification of NavQuest 600 Micro by LinkQuest Inc. for DVL, AsteRx1 by Septentrio for GPS, and MTi by Xsens for IMU.

Table 2 lists the simulation parameters for REMUS AUV given in (Presto, 2001) except for the movable mass $\overline{m}$, and two input gains b_x and b_m. Those values are arbitrarily chosen as $\overline{m} = 1(kg)$, $b_x = 0.001(m/\text{sec}\cdot V)$, and $b_m = 1/60(kg/\text{sec}\cdot V)$.

Simulation results using the LQR depth controller and the PD direction controller are shown in Fig. 6. For comparison, PD depth controller is not used intentionally. The 'O' indicates the starting point and the 'X' indicates the ending point. Fig. 6 shows that HAUV moved to position $(-100, 180)$ with seven zigzag movements.

Fig. 7 shows the variables related to the depth control by the LQR controller without elevator control. The surge (forward speed) of the HAUV starts from 0 m/s. According to the paper (Joo and Qu, 2015), the surge under no sea current is expected to be $0.3m/s$, but it keeps around 0.2 m/s until 6900 s because of the coming current. On the contrary, in the two zigzag movements after 6900 s, the forward speed is accelerated due to the influence of sea current.

Fig. 8 shows the control efforts of the LQR controller and its control results. The control inputs, u_x and u_b appear only briefly when HAUV changes direction, ie 1800 s, 6900 s, 7500 s and so on, and in most cases does not appear. As a result, the estimated values x_g^* and m_b^* changed suddenly and stabilize soon.

The PD direction controller controls the angle of the rudder effectively to control the direction of HAUV as shown in Fig. 9.

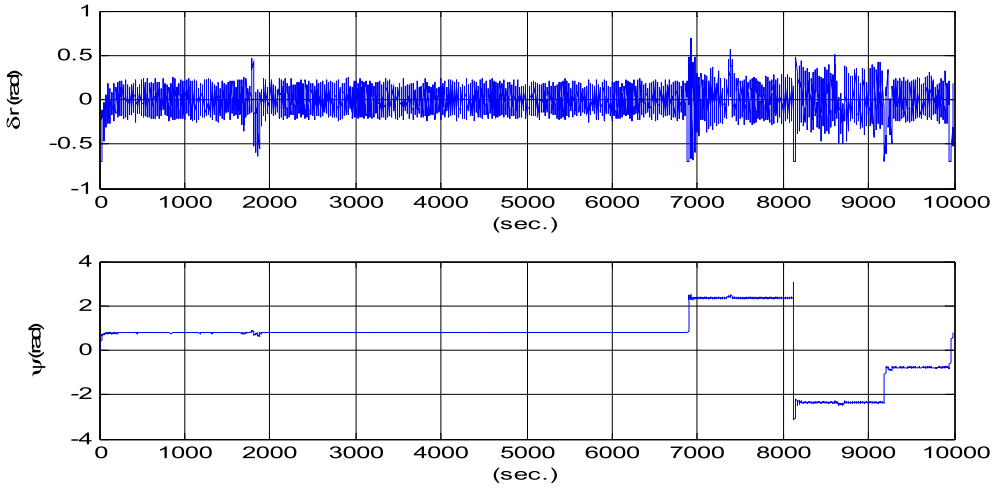

Fig. 9. Control effort of PD direction controller and its performance.

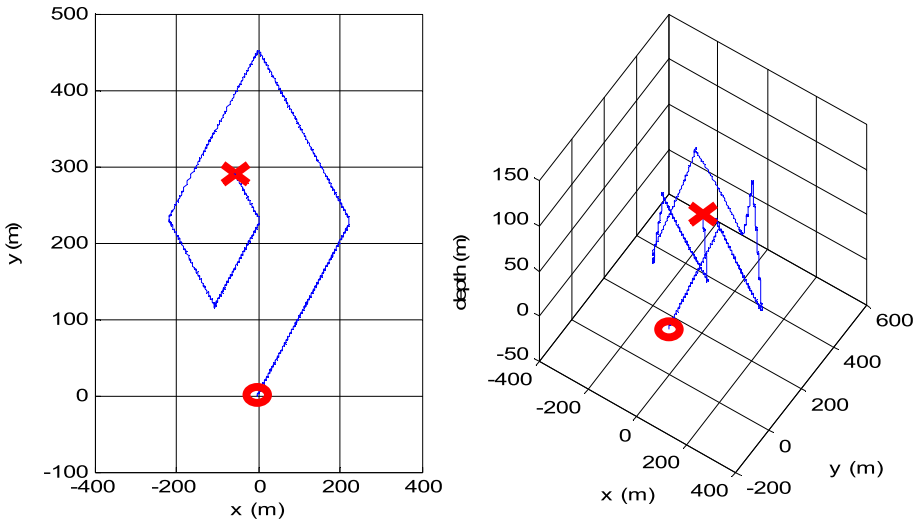

Fig. 10. The trajectory of HAUV with the proposed LQR/PD depth controller and PD direction controller.

Simulation results using the proposed LQR/PD depth controller and the PD direction controller are shown in Fig. 10. It shows that HAUV moved to position $(-30, 280)$ with nine zigzag movements. It can be seen that the PD elevator controller compensates the LQR controller, and as a result, the HAUV moves farther than the case of LQR controller alone.

In Fig. 11, the surge (forward speed) of the HAUV starts from 0 m/s, and is maintained at about 0.3 m/s with the progress of the gliding motion, which is consistent with the expected values in (Joo and Qu, 2015). It becomes about 0 m/s when the upward and downward movements are changed, Assuming that 0.15 m/s of sea current is pushed from the northeast, it can be seen that the surge is slowed down when the HAUV is heading north and the surge becomes faster when heading to the south.

Fig. 12 shows the control efforts of LQR controller and its results. The control inputs, u_x and u_b appear only briefly when HAUV changes direction, and in most cases does not appear. As a result, the estimated values x_g^* and m_b^* change quickly and stabilize soon.

The PD controller using the rudders can successfully control the direction of the HAUV as shown in Fig. 13, even if there is a relatively large sea current in comparison with the forward speed of the HAUV.

Fig. 14 shows the errors between actual values and estimated values, when the noise is removed on purpose to check the performance of the observer. The errors in the center of gravity and the buoyancy mass calculated by the reduced state observer occurs at

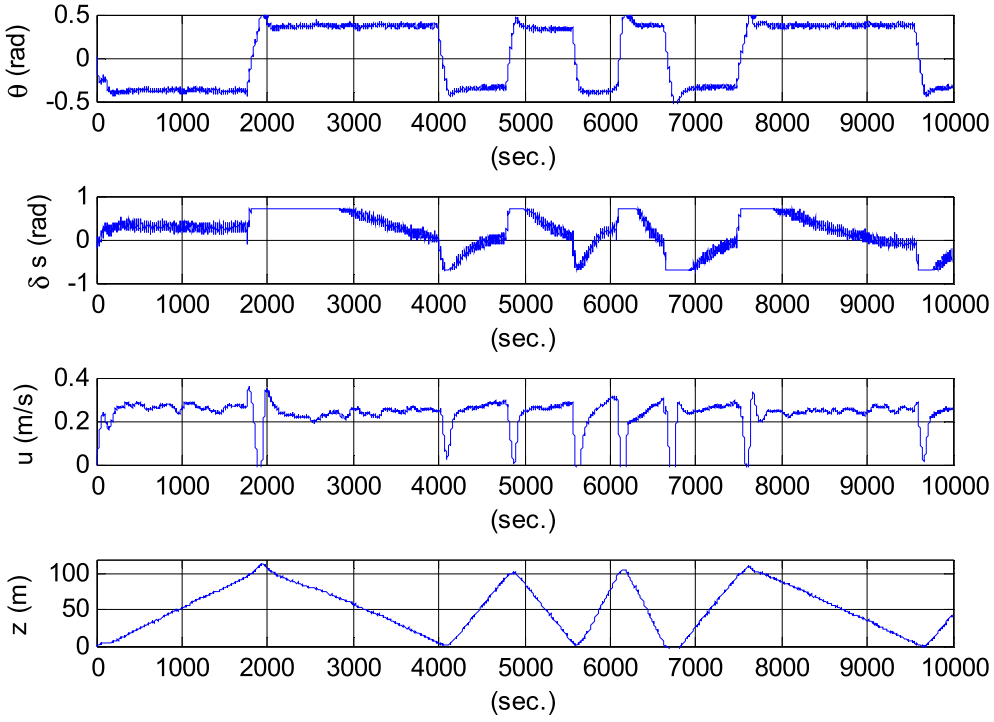

Fig. 11. Variables related to depth control by the LQR with PD elevator control.

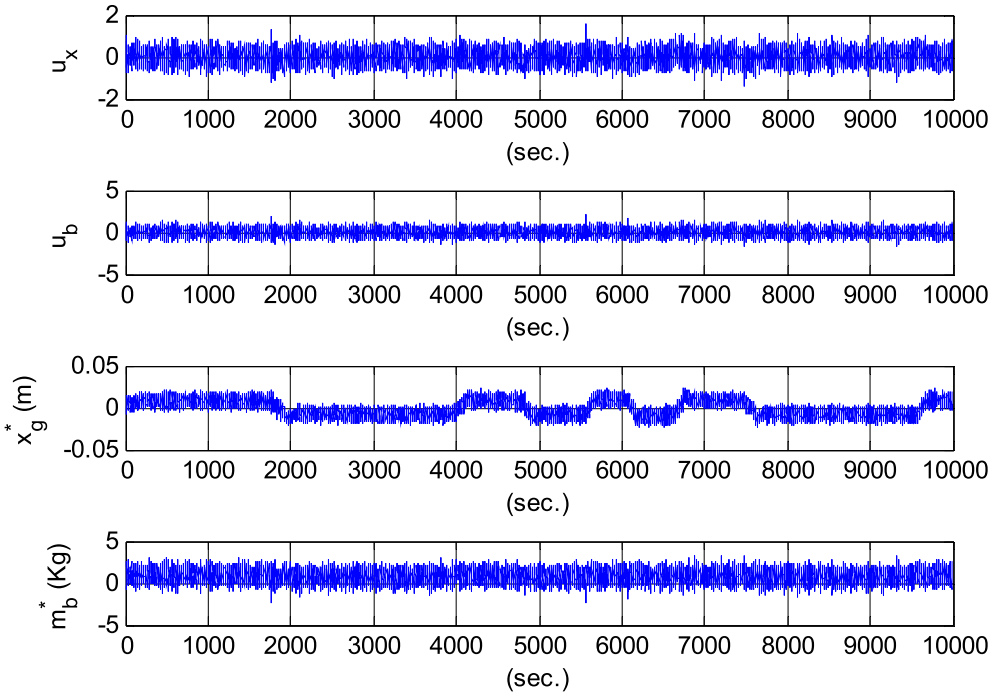

Fig. 12. Control effort of LQR and the change of estimated values.

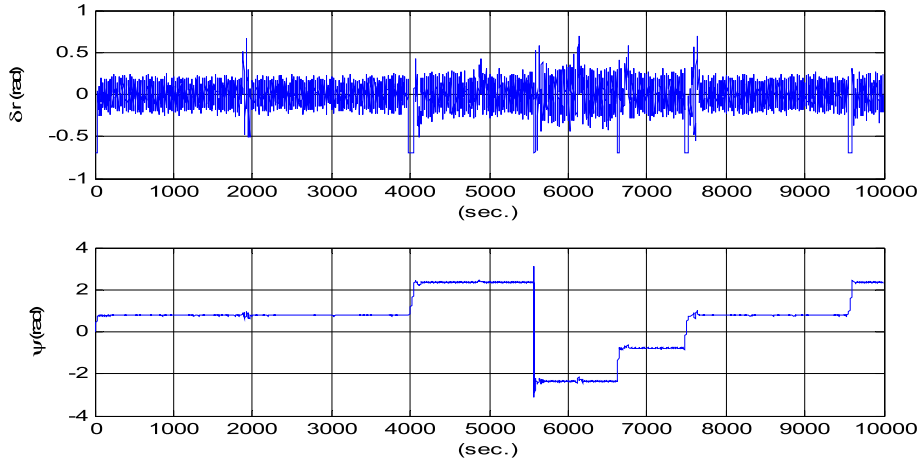

Fig. 13. Control effort of PD direction controller and its performance.

the beginning of the rise and fall movement of HAUV, but decreases rapidly with time.

6. Conclusion

The existing AUV advances with the propulsion of more than one propeller, which consumes a lot of energy and limits the operating time of the AUV. The underwater glider uses the center-of-gravity movement device and the buoyancy control device to obtain the propulsion force, which consumes small energy so that it operates for a long time and a long distance.

For HAUV, which combines the advantages of AUV and underwater glider, we proposed a depth and direction control scheme. The proposed controller was composed of an LQR controller to maintain zigzag vertical movement and two PD controllers to control elevator angle and rudder angle. The LQR controller controls the pumping speed of the buoyancy bag and the moving speed to locate the battery. One of the PD controller controls the elevator angle to assist the LQR controller, and the other controls the rudder angle to adjust the direction of the underwater glider.

A reduced order Luenberger observer was adopted to estimates the center of gravity of the glider and the buoyancy mass which were essential but could not be measured.

Mathematical simulation using Matlab proved that the proposed control scheme maintained the attitude and surge speed under the influence of sea current, while the conventional LQR only controller showed surge decrease casusing the shortening of forward distance in the same situation. It is due to the proposed PD controller of tail wings compensating for the pitch angle variation due to sea current, but the tail wings has not been used in HAUV until now.

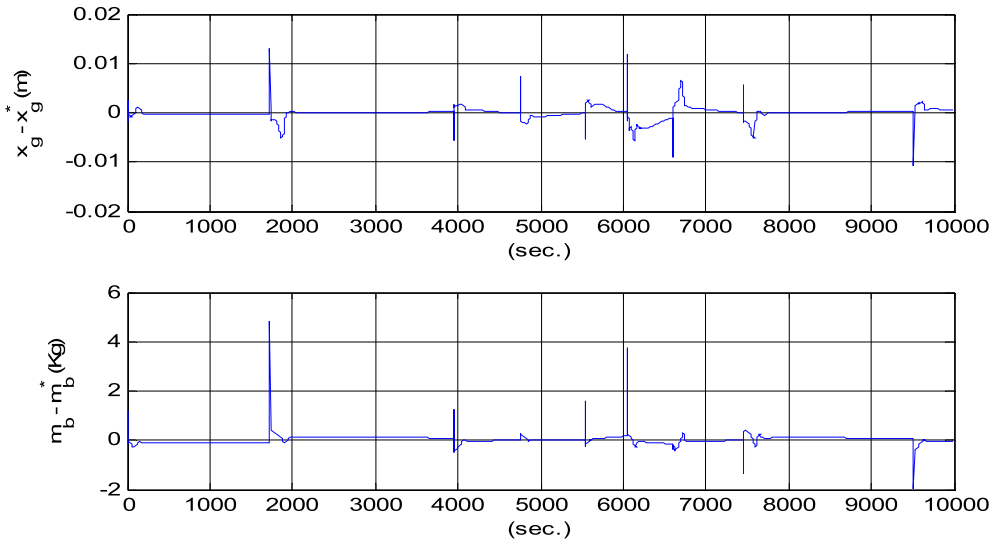

Fig. 14. Errors in estimated values from a reduced order observer.

Acknowledgements

This journal was supported by the Korean National Research Foundation Grant. (NRF-2016R1D1A3A03917039)

References

Alvarez, A., 2010. Redesigning the SLOCUM glider for torpedo tube launching. IEEE J. Ocean. Eng. 35 (24), 984–991.

Ballard, Robert D., 1993. The MEDEA/JASON remotely operated vehicle system. Deep Sea Res. Oceanogr. Res. Pap. 40 (8), 1673–1687.

Eriksen, Charles C., Osse, T. James, Light, Russell D., Wen, Timothy, Lehman, Thomas W., Sabin, Peter L., Ballard, John W., Chiodi, Andrew M., 2001. Seaglider: a long-range autonomous underwater vehicle for oceanographic research. IEEE J. Ocean. Eng. 26 (4), 424–436.

Fossen, Thor I., 1994. Guidance and Control of Ocean Vehicles. John Wiley & Sons, Ltd.

Fossen, Thor I., 2011. Handbook of Marine Craft Hydrodynamics and Motion Control. John Wiley & Sons, Ltd.

Hagen, Per Espen, Størkersen, Nils, Marthinsen, Bjørn-Erik, Sten, Geir, Vestgård, Karstein, 2008. Rapid environmental assessment with autonomous underwater vehicles - examples from HUGIN operations. J. Mar. Syst. 69, 137–145.

Javadi-Moghaddam, J., Bagheri, A., 2010. An adaptive neuro-fuzzy sliding mode based genetic algorithm control system for under water remotely operated vehicle. Expert Syst. Appl. 37 (1), 647–660.

Joo, Moon G., Qu, Zhihua, 2015. An autonomous underwater vehicle as an underwater glider and its depth control. IJCAS 13 (5), 1212–1220.

Joo, Moon G., Woo, Him-Chan, Son, Hyeong-Gon, 2017. Depth control of underwater glider using reduced order observer. IEMEK J. Embed. Syst. Appl. 12 (5), 311–318.

Jun, Bong-Huan, Park, Jin-Yeong, Lee, Fill-Youb, Lee, Pan-Mook, Kim, Kihun, Lim, Young-Kon, Oh, Jun-Ho, 2009. Development of the AUV 'ISiMI' and a free running test in an ocean engineering basin. Ocean Eng. 36, 2–14.

Presto, Timothy, 2001. Verification of a Six-Degree of Freedom Simulation Model for the REMUS Autonomous Underwater Vehicle. M. S. thesis. Applied ocean science and engineering, MIT & WHOI.

Sherman, Jeff, Davis, Russ E., Owens, W.B., Valdes, J., 2001. The autonomous underwater glider 'Spray'. IEEE J. Ocean. Eng. 26 (4), 437–446.

Shim, Hyungwon, Jun, Bong-Huan, Lee, Pan-Mook, Baek, Hyuk, Lee, Jihong, 2010. Workspace control system of underwater tele-operated manipulators on an ROV. Ocean Eng. 37 (11–12), 1036–1047.

Wang, Shu-Xin, Sun, Xiu-Jun, Wang, Yan-Hui, Wu, Jian-Guo, Wang, Xiao-Ming, 2011. Dynamic modeling and motion simulation for a winged hybrid-driven underwater glider. China Ocean Eng. 25 (1), 97–112.

Webb, Douglas C., Simonetti, Paul J., Jones, Clayton P., 2001. SLOCUM: an underwater glider propelled by environmental energy. IEEE J. Ocean. Eng. 26 (4), 447–452.

Xue, Dong-Yang, Wu, Zhi-Liang, Wang, Yan-Hui, Wang, Shu-Xin, 2018. Coordinate control, motion optimization and sea experiment of a fleet of Petrel-II gliders. Chin. J. Mech. Eng. 31 (17), 1–15.